Influence of CO_2 Dissolution and Asphaltene Precipitation on Oil PVT and Recovery

Maryam Khosravi[1*], Behzad Rostami[2], Long Nghiem[3]
1- Research Institute of EOR (NIOC), Tehran, Iran.
2- Petroleum University of Technology, Tehran, Iran.
3- Computer Modeling Group, Calgary, Canada.

E-mail: ***Khosravi@nioc.rtd.ir***

Abstract
CO_2 injection is one of the most common enhanced oil recovery methods, but it may change the reservoir fluid properties and cause some problems such as asphaltene precipitation, resulting in reduction of injectivity and productivity of oil wells, and plugging wellbore and production facilities.
The objective of this work is modeling oil PVT and asphaltene precipitation through the compositional simulator using experimental data from Srivastava et al[1]. The process of CO_2 injection is studied and the effect of CO_2 dissolution and asphaltene precipitation are investigated on oil recovery, oil mass density and viscosity.
Results of numerical experimentation indicate that the maximum amount of precipitation occurs around the saturation pressure and concentration of the fluid. Results indicate that both asphaltene precipitation and CO_2 dissolution act in parallel in order to reduce the oil viscosity, but they work against each other in the case of density. Asphaltene precipitation causes an upgrade in oil properties which might be in favor of either "higher recovery" or "higher rate of pore plugging and permeability reduction"; two opposing phenomena. For different oils and different reservoirs, one of these two phenomena could be dominant.

Keywords: CO_2 injection, Asphaltene precipitation, Asphaltene Deposition

1. Introduction
After initial waterflooding, many light and medium oil reservoirs are subjected to miscible or near-miscible CO_2 or hydrocarbon flooding for enhanced oil recovery. Under the specific conditions of pressure, temperature and oil composition, the CO_2 becomes miscible with the oil and causes the residual oil to swell, and reducing the viscosity. One of the major problems that confront reservoir/ production engineers considering a miscible CO_2 flood for a field is the need to assess the likelihood of asphaltene precipitation and consequent oil recovery and monetary losses. To do this, experimental studies or modeling techniques are initiated to determine "when" and "how much" asphaltene will be precipitated.

In this paper, the term "precipitation" refers to the formation of the asphaltene precipitate as a result of thermodynamic equilibrium, and "deposition" refers to the settling of the precipitated asphaltene onto the rock surface in a porous medium.

Inside the reservoir, after precipitation has occurred, the asphaltene precipitate can remain in suspension and flow within the oil phase, or can deposit onto the rock surface. The deposited asphaltene may cause plugging of the formation and alteration of rock wettability (from water-wet to oil-wet). Many thermodynamic models, to describe the behavior of asphaltene precipitation and deposition, have been reported in the literature. Among them are the liquid solubility model by Hirshberg et al. (1984), a thermodynamic colloidal model by Leontarities and Mansoori (1987), a pure solid model by Nghiem (1993), a colloidal activity coefficient model by Zhou et al. (1996) and a thermodynamic micellization model by Pan and Firoozabadi (1998) [2-6].

This paper focuses on the compositional simulation of asphaltene based on Nghiem's model. We concentrate on CO_2 injection in the Weyburn reservoir and examine the effect of operating pressure and CO_2 concentration on asphaltene flocculation/precipitation. In addition, oil PVT and recovery have been analyzed under different situations.

2. Data Evaluation

A study on asphaltene precipitation due to CO_2 injection for Weyburn reservoir fluids has been reported by Srivastava et al. [1]. PVT cell was used for determining the onset of asphaltene flocculation and measuring the amount of asphaltenes flocculated. The extent of asphaltene deposition was also assessed through coreflood experiments and through an x-ray computer aided tomography (CAT) scanning visualization experiment. Oil composition and its physical properties are shown in Table 1 and Table 2.

3. Asphaltene Equations

The precipitated asphaltene is modeled as a pure solid. This model has previously been presented and validated for description of asphaltene precipitation behavior over a wide range of pressure, temperature and composition conditions [7, 8]. The pure solid is described within the framework of the EOS model by splitting the heaviest pseudo component in the oil characterization into the non-precipitating component (C30+A) and a precipitating component (C30+B). These two components have identical critical properties and acentric factors, but different interaction parameters with light components in the system. The precipitating component may be considered to include asphaltene and resin molecules.

Table 1. Physical properties of Weyburn oil

Saturation pressure, kpa	2300
Density, kg/m^3	833.5
Formation volume factor	1.088
GOR, m^3/m^3	1.076
^oAPI	19.2

Table 2. Composition of Weyburn oil

Component	Composition
N2 to C1	5.50
CO2	0.34
C2 to C3	9.77
IC4 to NC5	12.76
C6 to C9	29.93
C10 to C19	28.85
C20 to C29	9.47
C30A+	1.94
C30B+	1.44
MW C30B+	616.1357
Sg C30B+	1.3121
Saturation pressure, kpa	2300
Density, kg/m^3	833.5
Formation volume factor	1.088
GOR, m^3/m^3	1.076
^oAPI	19.2
Weight % asphaltene of stock tank oil	5.3 %
Weight % asphaltene at 16 MPa, 59 °C and CO_2 mole % 53.5	0.93%

Some part of B fraction precipitates into solid phase as asphaltene or converts to S_1 phase through thermodynamic equilibrium (Equation 1).

Generation of S_1 is the first phase of deposition. Some parts of S_1 convert to S_2 through Equations (2) and (3). This phase is known as flocculated asphaltene, which is in fact aggregations of precipitated asphaltene molecules. Some part of flocculated asphaltene deposits on the rock surface as deposited asphaltene (Equation 4) and cause permeability and porosity to reduce.

3.1 Asphaltene Precipitation Model

When asphaltene is included, equilibrium equations could be solved. C30+ is in equilibrium with asphaltene solid phase S_1. The solid fugacity, f_{S1}, is given by:

$$\ln f_{S_1} = \ln f_{S_1}^{*} + \frac{v_{s_1}\left(p - p^{*}\right)}{RT} \qquad (1)$$

It will show that complete thermodynamic reversibility and any precipitated solid S_1 would go back into the solution when the system is returned to a state outside the asphaltene precipitation envelope [9].

3.2 Asphaltene Flocculation Model

Irreversibility of solid precipitates is modeled by allowing solid S_1 to be transformed via a simple reversible chemical reaction into another solid, S_1. This can be viewed as the flocculation of smaller asphaltene particles into larger aggregates. The reaction may be written as follows:

$$S_1 \longleftrightarrow S_2 \qquad (2)$$

The reaction rate for the formation of S_2 is:

$$r = k_{12} C_{S_1,o} - k_{21} C_{S_2,o} \qquad (3)$$

Note that S_2 can go back into the solution by first becoming S_1 through the reverse reaction, and then dissolving into the oil phase through thermo-dynamic equilibrium.

3.3 Asphaltene Deposition Model

An equation relating asphaltene deposition rate to the primary physical deposition processes (adsorption, pore throat plugging and re-entrainment) was presented by Wang and Civan [10]. In fact, they modified modified Gruesbeck and Collin's theory of plugging and non-plugging [11]. The discretized form of the deposition rate equation is:

$$\frac{V_{S_2^d}^{n+1} - V_{S_2^d}^{n}}{\Delta t} - \alpha C_{S_2^f}^{n+1} \phi^{n+1} + \beta V_{S_2^d}^{n+1}\left(v_o^n - v_{cr,o}\right) - \gamma . u_o^n C_{S_2^f}^{n+1} = 0 \qquad (4)$$

The surface deposition rate coefficient α is a positive constant and is dependent on the rock type. The entrainment rate coefficient β is set to zero when the interstitial velocity is less than critical velocity. The pore-throat plugging coefficient γ is set to zero if the average pore throat diameter is larger than some critical values [8].

When asphaltene is included, Equation (5) is added to the flow equations for deposited solid S_2 and transport of solid S_2.

$$\Delta T_o^m y_{is_2}{}^m \left(\Delta p^{n+1} - \gamma_o^m \Delta D\right) + V\phi S_o r + q_i^{n+1} - \frac{V}{\Delta t}\left(N_i^{n+1} - N_i^n\right) = 0, i = 1,..,n_c \qquad (5)$$

The unknowns are pressure, moles of hydrocarbon and water components, K-values, moles of S_1, moles of S_2 and moles of deposited S_2.

3.4 Construction of a Phase Diagram

In order to construct a phase diagram, it is necessary to perform several flash calculations at identified pressures for different fractions of CO_2. Four-phase (V-L1-L2-S) flash calculation has been performed at different pressures between 100 and 70000 kpa. From the output results, it is possible to find out the mole fraction of different phases. Finally, by locating these whole points together in one diagram, the phase diagram of the oil can be achieved as shown in Fig. 1.

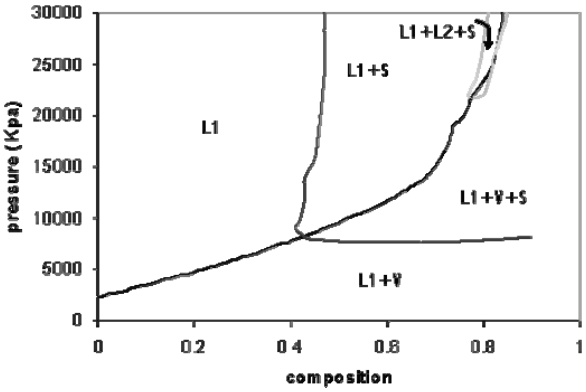

Figure 1. Phase diagram of Weyburn oil

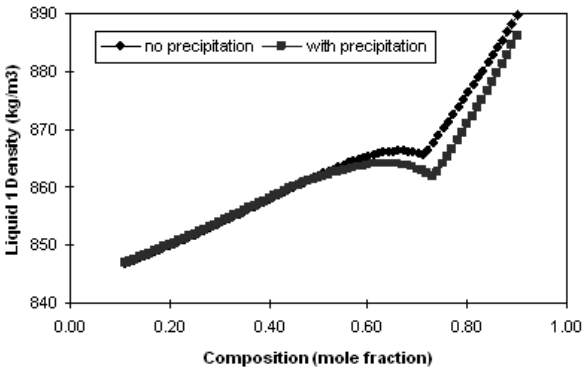

Figure 2. Oil density versus CO_2 composition at 16 Mpa

4. Analysis of Oil Behavior against CO_2 Composition and Pressure

Alternation of the oil density by CO_2 injection is shown in Fig. 2. The oil density increases as CO_2 concentration increases in the system. A sharp increase can be observed after the saturation concentration of CO_2. Density of the oil can be calculated by dividing molecular weight to molar volume. Before the system becomes two phases, both molecular weight and molar volume of the oil decrease (molar volume decreases, because the increase in mole numbers is faster than the oil volume increase due to volumes' real behavior in the mixing process), but molar volume decreases faster and, as a result, density increases. This behavior has been observed in oils with one component (for example C_{10}), therefore it is not because of composition variation. After a while, the rate of reduction of molar volume decreases because the system is going to be saturated with CO_2. This could be reflected as a local minimum in density curve.

When vapor phase is generated, molar volume and molecular weight of the oil increase (some components such as dissolved CO_2 and light hydrocarbons go to the gas phase, while decrease in mole numbers is faster than oil volume reduction), but molecular weight increases faster. In other words, CO_2 increases oil density by withdrawing the light components of oil. Therefore, CO_2 injection is dominated by vaporizing.

Fig. 3 shows when CO_2 dissolves in oil in the absence of vapor phase, oil viscosity decreases. But, in the presence of the vapor phase, oil viscosity increases because of vaporization of oil light fractions. Fig. 2 and 3 indicate that asphaltene precipitation causes reduction in oil density and viscosity, which are in favor of recovery.

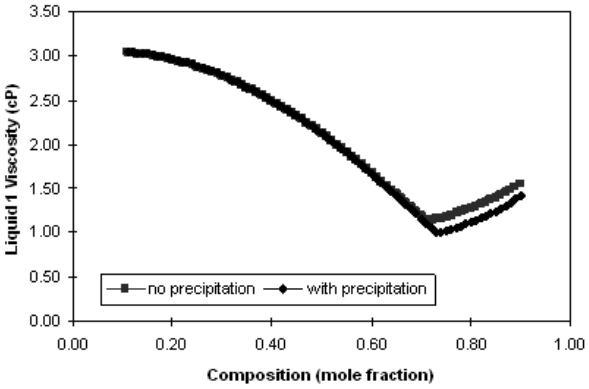

Figure 3: Oil viscosity versus CO_2 composition at 16 Mpa

This test has been repeated for different pressures. As the pressure increases, the amount of weight percentage of precipitated asphaltene increases. When data are converted to mass (Fig. 4), it can be observed that the mass of precipitated asphaltene increases and at a special pressure (near MMP) this amount remains constant. Moreover, as the pressure increases, (process becomes more miscible) changes in phase variation become sharper and changes in

oil density and viscosity become more pronounced. This behavior is shown in Figs. 5 and 6.

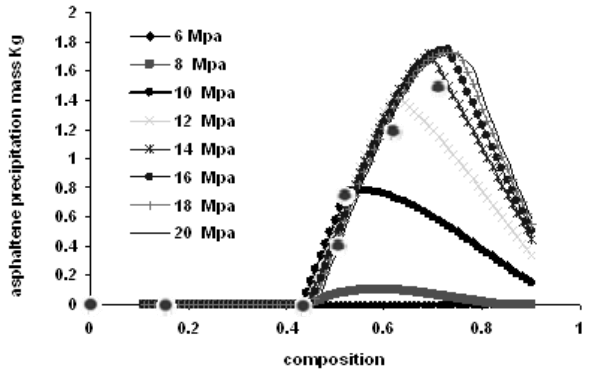

Figure 4. Asphaltene precipitated mass (kg) versus composition

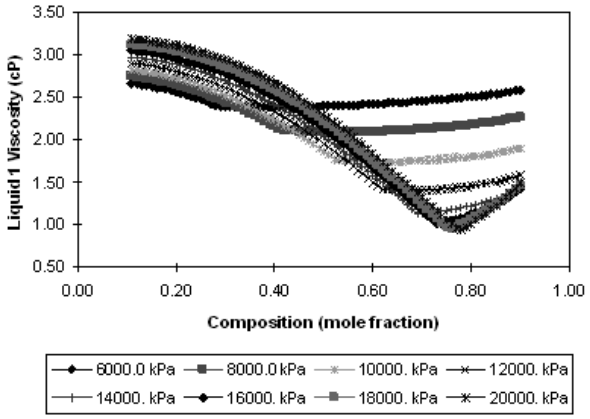

Figure 5. Oil viscosity changes versus CO_2 composition and pressure

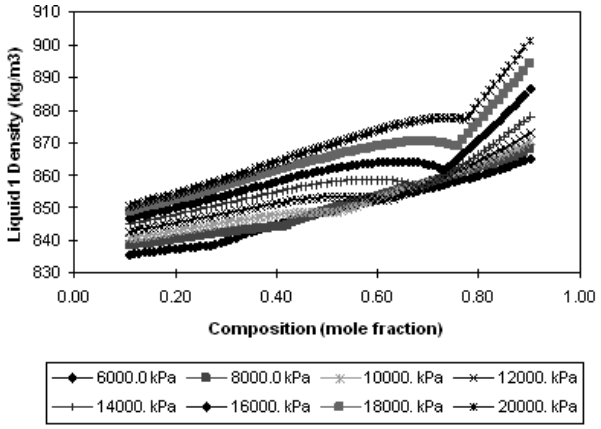

Figure 6. Oil density changes versus CO_2 composition and pressure

5. Investigation of CO_2 Process in Porous Media

The model used in this study has been suggested by Nghiem and Coombe [7] for investigation of asphaltene precipitation and deposition in a core. The model is 1-D with no gravity forces at this stage and the length of the core is larger than the length of the miscibility zone. Dimensions of the system are chosen such that time becomes equal to the injected pore volume. CO_2 is injected continuously into the injection well (first grid) and oil is produced from the production end (last grid). In order to avoid production due to pressure gradient, the pressure of the reservoir and production well have been kept equal and constant. Core properties and key operating conditions are given in Table 3.

Table 3. Model properties

Pore volume	1.668E-3 m^3
Porosity	0.3
Permeability	500 md
Reservoir Pressure	16 Mpa
Reservoir temperature	59°c
Production well pressure	16 Mpa
Injection flow rate	1.668E-3 m^3

In this study, injection is "near miscible" (MMP is 16375 kpa). When CO_2 saturation reaches a special value, the gas phase starts to liberate within the system. In many aspects oil behavior should be different before and after gas phase generation. Hence, the process should be investigated ahead of the gas front and behind it.

For a better understanding of the process, CO_2 fraction of oil, and gas saturation are shown in all figures. In addition, the miscibility zone is identified as the area where solvent concentration varies from 10 to 90 percent.

5.1. CO_2 Effect on Oil Properties

Fig. 7 shows the accumulation of the gas phase near the injection well. As the gas front goes forward, CO_2 diffuses into the oil and changes its properties and also causes asphaltene precipitation. The concentration of CO_2 increases to a maximum on the gas phase front which is the saturation

concentration of the system. When gas phase generation starts at a special point, interfacial tension (IFT) begins to increase and the tendency of CO_2 to dissolve in oil reduces. As a result, the CO_2 concentration in oil declines while its global mole fraction increases.

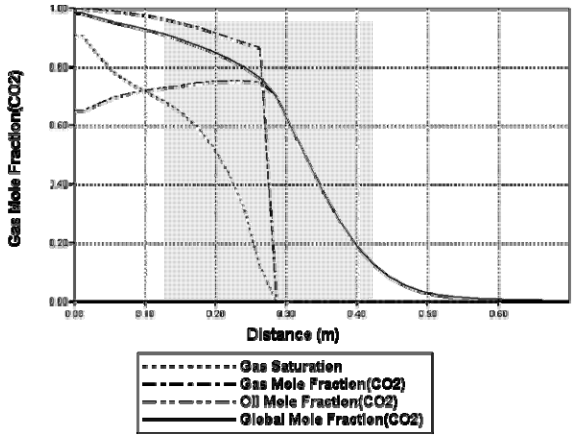

Figure 7. Profiles of CO_2 fraction and gas saturation versus distance at 0.4 PV injection

Ahead of the gas front, CO_2 causes viscosity reduction and a gentle increase in density because of CO_2 dissolution in oil. When the gas phase generates, oil viscosity and density increase considerably, because of the vaporization of oil light components. Therefore, the remaining oil behind the front will be extremely dense and viscous. Figure 8 illustrates the change in oil viscosity and density, which is entirely in line with the literature.

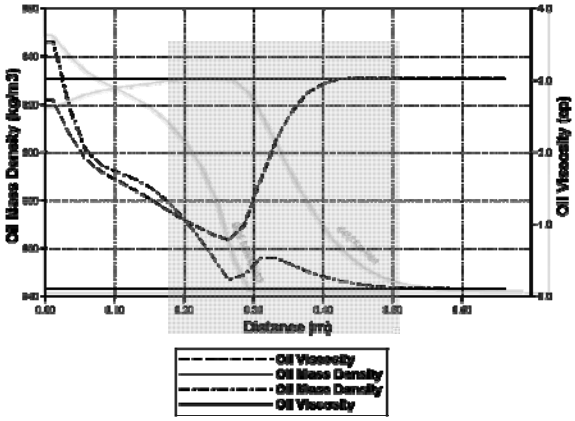

Figure 8. Profiles of oil viscosity and density versus distance at 0.4 PV injection

Fig. 9 indicates that asphaltene starts to precipitate when CO_2 concentration reaches a critical value. The total amount of asphaltene which comes out of the liquid phase is named "total asphaltene" and is equal to a summation of the remained precipitation asphaltene, flocculated asphaltene and deposited asphaltene of the system. Precipitated asphaltene is solid S_1. Some part of this phase converts to solid S_2 and is suspended in the liquid phase as aggregated structure. The converted S_1 or S_2 phase is named "flocculated asphaltene". Again some part of S_2 deposits on the rock surfaces and some parts are suspended in the liquid phase. Hence, flowing asphaltene would be a combination of precipitated and flocculated asphaltene. What remains from solid S_1 in the system is called "precipitated asphaltene" in Fig. 9.

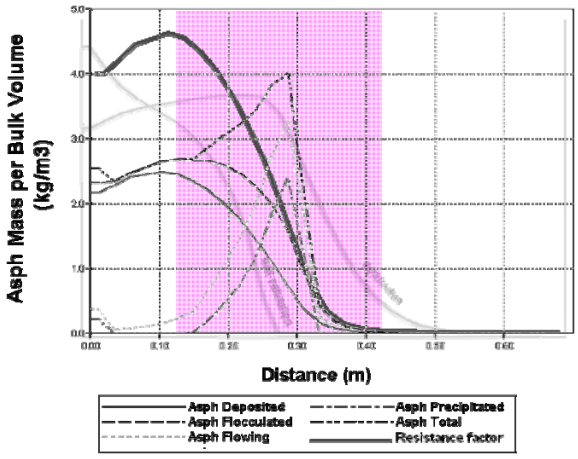

Figure 9. Asphaltene profiles versus distance at 0.4 PV injection

S_1 and S_2 are continually generated and consumed within the system, but when the CO_2 concentration in oil reaches its saturation value, the rate of production of S_1 and S_2 are higher than the consumption. In contrast, behind the gas front, where oil becomes dense and its structure is similar to asphaltene's structure, asphaltene prefers to remain in oil and the rate of consumption in this area would be higher. As a result, behind the front the amount of precipitated asphaltene reaches zero

where flocculated and deposited asphaltene increase. Fig. 9 also illustrates how the resistance factor changes in the core and how formation damage is serious near the injection well.

Fig. 10 shows composition variation within the core. It explains how lighter cuts of oil (C2 to C9) vaporized into the gas phase. Also, it can be seen that the remained oil behind the front is dense due to a high fraction of C20+ (C20-C29, C30+A, C30+B).

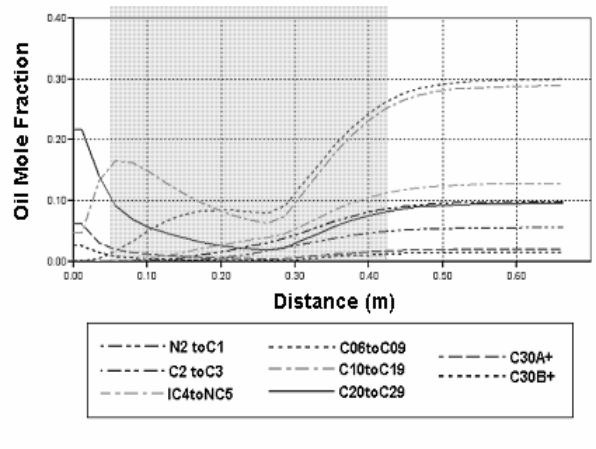

Figure 10. Composition variation in oil phase at 0.4 PV injection

5.2 Asphaltene Effect on Oil Properties

In order to find out the real effect of asphaltene, the results are compared with the results of a similar model with no precipitation or depositions in Fig. 11. As expected, behind the gas front, as asphaltene goes out of the system, viscosity and density decrease. However, ahead of the gas front opposite behavior is observed. Evaluation of oil phase behavior is important because the amount of the oil saturation is high in this area and it could affect the recovery. In this zone, when asphaltene comes out of oil more CO_2 can dissolve into the oil and it becomes a competition between gas and asphaltene for dissolution into oil. In the case of viscosity, asphaltene precipitation and CO_2 solution act in parallel; However, in the case of density they work against each other. Figure 11 illustrates that CO_2 affects oil behavior more than asphaltene. It should be noted that it can be different in the case of different oils with different asphaltene contents and for each system the whole comparisons should be repeated. The effect of asphaltene precipitation on the recovery was negative because of the viscosity increase ahead of the gas front (oil bank) and the porosity (and as a result, permeability) decrease due to asphaltene deposition.

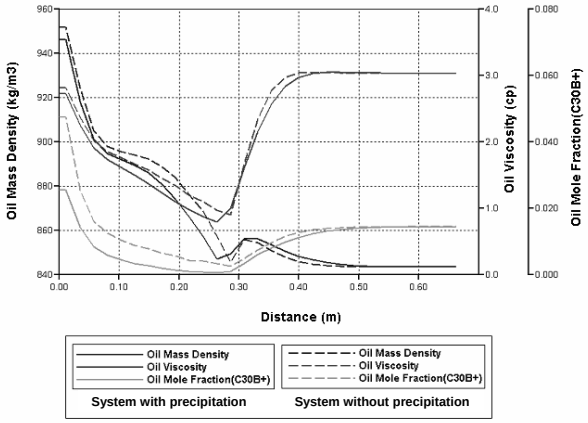

Figure 11. Effect of asphaltene precipitation on oil density and viscosity

Conclusions

Asphaltene deposition was modeled for CO_2 injection using a compositional simulator. Based on the presented results the following conclusions are obtained:

1. Asphaltene and CO_2 work against each other in the case of density; solution of CO_2 causes the density to increase but asphaltene precipitation decreases the oil density.
2. Asphaltene and CO_2 have the same effect in the case of viscosity. The solution of CO_2 and asphaltene precipitation cause viscosity to decrease.
3. Usually the maximum amount of precipitation occurs around the saturation composition of the fluid. Above this composition, liberation of gas from the oil changes the solubility parameter of the liquid phase and allows redissolution of the precipitated asphaltene. This phenomenon can be considered such a competition between asphaltene and CO_2 to solve into oil.

4. Athough asphaltene precipitation causes an upgrade in oil PVT, asphaltene deposition may cause permeability reduction. In this study, permeability reduction was dominant and the recovery was reduced.

Acknowledgment

I would like to thank the National Iranian Oil Company (NIOC) for its support and encouragement throughout my research project. I thank Dr. Rostami for his helpful advice and his incredible patience with me.

Nomenclature

C_{sf}	concentration of solid in the oil phase [ppm (μg/g)]
$\hat{C}_{sf}$	concentration of precipitated asphaltene in oil phase [m^3/m^3]
f_s	solid fugacity [kpa]
f_s^*	reference solid fugacity [kpa]
g	gravity acceleration [m/s^2]
n_c	number of components in hydrocarbon phases
N_i	moles of component i per bulk volume
p^*	reference pressure [kpa]
q_i	molar injection/production rate of component i [kmol/day] [$kmol/m^3$ day]
R	gas constant [8.314 kpa m^3/kmol K]
R_f	permeability reduction factor
S_j	saturation of phase j
T_j	transmissibility of phase j [kmol/kpa/day]
u_o	oil Darcy velocity [m/s]
$v_{cr,o}$	critical pore velocity of oil [m/s]
v_o	pore velocity of oil [m/s]
v_s	solid molar volume [m^3/kmol]
V	gridblock volume [m^3]
γ_j	$\tilde{\rho}_j g$; gradient of phase j (j = o,g,w) [kpa/m]
y_{ij}	mole fraction of component i in phase j (j = o,g,s)
y_{isf}	mole fraction of solid in suspension in oil phase

References

[1] Srivastava, R.K., Huang, "S.S., Dyer, S.B. and Mourits, F.M. 1995. Quantification of asphaltene flocculation during miscible CO_2 flooding in the Weyburn Reservoir". J. Can. Petrol. Technol. 34, 31-42.

[2] Hirschberg, A., deJong, L.N.J., Schipper, B.A., and Meijer, J.G. 1984. "Influence of temperature and pressure on asphaltene flocculation". Paper SPE 11202, June.

[3] Leontarities, K.J., and Mansoori G.A. 1987. "Asphaltene flocculation during oil production and processing: A thermodynamic colloidal model". Paper SPE 16258, Presented at SPE Symp. on oil field Chem., San Antonio.

[4] Nghiem, L.X., Hassam, M.S., Nutakki, R., George, A.E.D., 1993. "Efficient Modeling of asphaltene precipitation". Paper SPE 26642 presented at the SPE Conference and Exhibition, Houston, TX, 3-6 October.

[5] Zhou, X., Thomas, F.B., and Moore, R.G. 1996. "Modeling of solid precipitation from reservoir fluids". J. Can. Petrol. Technol. 35, 37-45.

[6] Pan, H., and Firoozabadi, A., 1998. "Thermodynamic micellization model for asphaltene aggregation and precipitation in petroleum fluids". SPE Production & Facilities, May: 118-127.

[7] Nghiem, L.X., and Coombe, D.A. 1997. "Modeling asphaltene precipitation during primary depletion". SPE Journal. 2(6), 170-6.

[8] Kohse, B.F., Nghiem, L.X., Maeda, H., and Ohno, K. 2000. "Modeling phase behavior including the effect of pressure and temperature on asphaltene precipitation". Paper SPE 64465, Presented at SPE Asia Pacific Oil and Gas Conference and Exhibition, Brisbane, Australia, 16-18 October.

[9] Kohse, B.F., and Nghiem, L.X. 2004. "Modeling asphaltene precipitation and deposition in a compositional reservoir". Paper SPE 89437 presented at SPE/DOE Fourteenth Symposium on Improved Oil Recovery, Tulsa, Oklahoma, U.S.A., 17–21 April.

[10] Wang, S. and Civan, F. 2001. "Productivity decline of vertical and horizontal wells by asphaltene deposition in petroleum reservoirs". Paper SPE 64991, Presented at SPE International Symposium on Oilfield Chemistry, Houston, TX, 13-16 February.

[11] Gruesbeck, C. & Collin's, R. E.: "Entrainment & Deposition of Fine Particles in Porous Media", Soc. Petrol. End. J. (Dec. 1982) 847-856.